Electronic Supplementary Material (ESI) for Journal of Materials Chemistry B

Electronic Supplementary Information

Gold nanoparticles decorated with ferrocene derivative as a potential shift-based transducing system with interest for sensitive immunosensing

Abdelmoneim Mars,[a,b] Claudio Parolo,[a] Noureddine Raouafi,*[b] Khaled Boujlel[b] and Arben Merkoçi*[a,c]

** Prof. A. Merkoçi, Prof. N. Raouafi*

[a] Nanobioelectronics & Biosensors Group, Catalan Institute of Nanotechnology (ICN, Campus de la UAB -Edifici Q (ETSE) - 2ª planta, 08193 Bellaterra, Barcelona, Spain. Fax: +34935868020; Tel: +34935868014. E-mail: arben.merkoci@icn.cat

[b] University of Tunis El-Manar, Faculty of Science, Laboratory of Analytical Chemistry and Electrochemistry, Campus Universitaire de Tunis El-Manar 2092, Tunis, Tunisia. Fax: +21671883424; Tel: +21671872600, Email: n.raouafi@fst.rnu.tn

[c] ICREA, Barcelona, Spain.

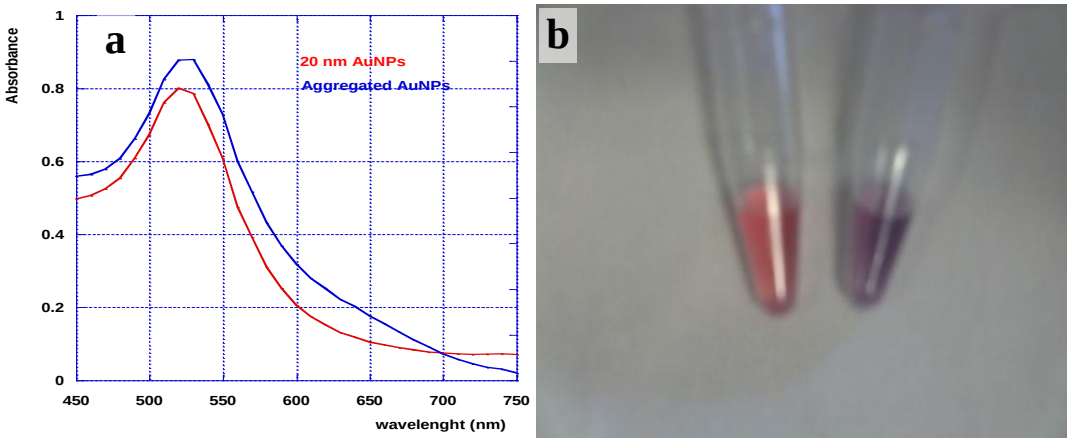

Fig. S1 (a) AuNPs SPR band change in UV-visible spectroscopy before (red) and after (bleu) the FcD addition; (b) The AuNPs colour change during the aggregations red (before) and purple (after).

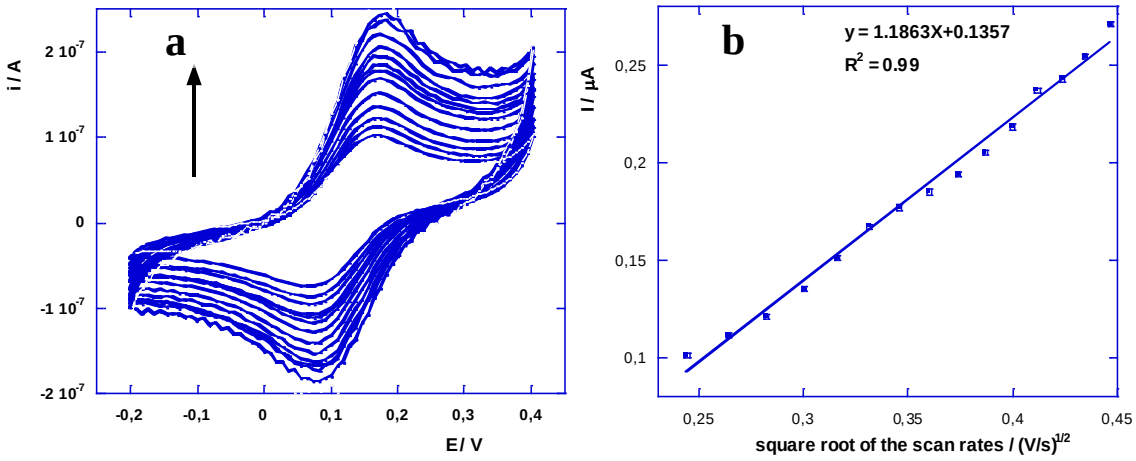

Fig. S2 (a) Cyclic voltammograms of the HIgG immunosensor without the analyte at different scan rates from 50 to 170 mV/s in mQ water, (b): the linear dependence of oxidation peak current on the square root of the scan rate.

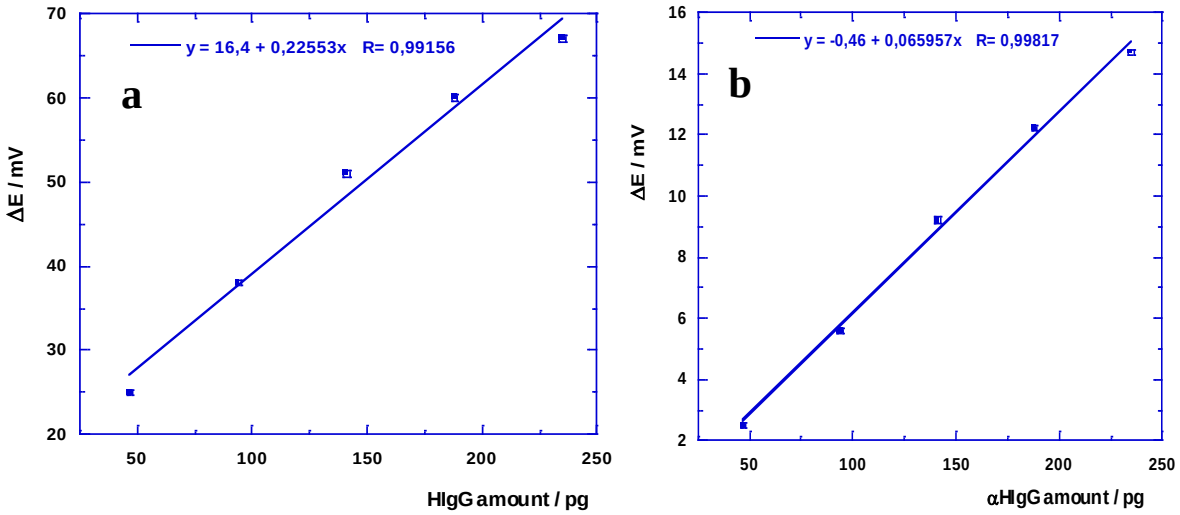

Fig. S3 Oxidation peak potential variation versus the protein amounts: (a) HIgG and (b) GIgG

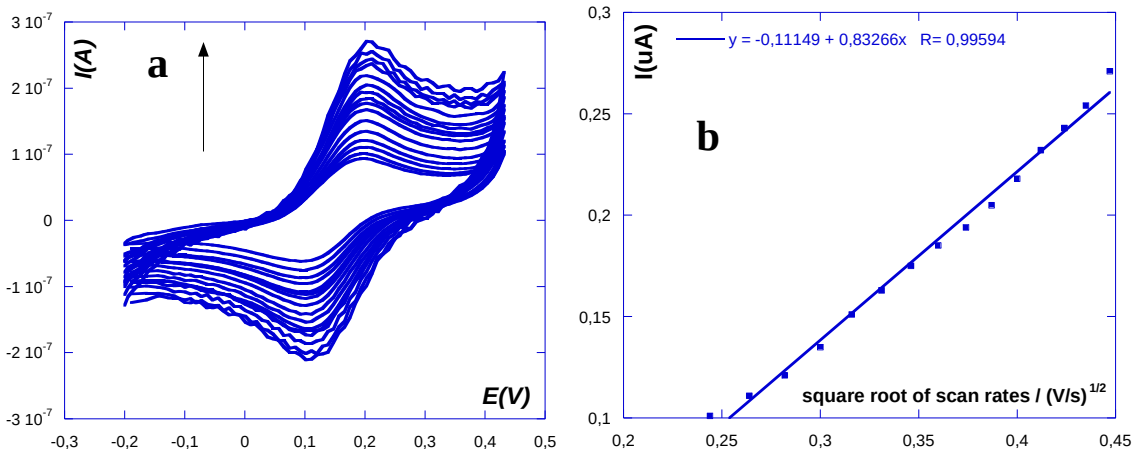

Fig. S4.1 (a) CV curves of the immunosensor with 47 ng/mL of HIgG at different scan rates from 50 to 200 mV/s in mQ water, (b): the linear dependence of oxidation peak current on the square root of the scan rates.

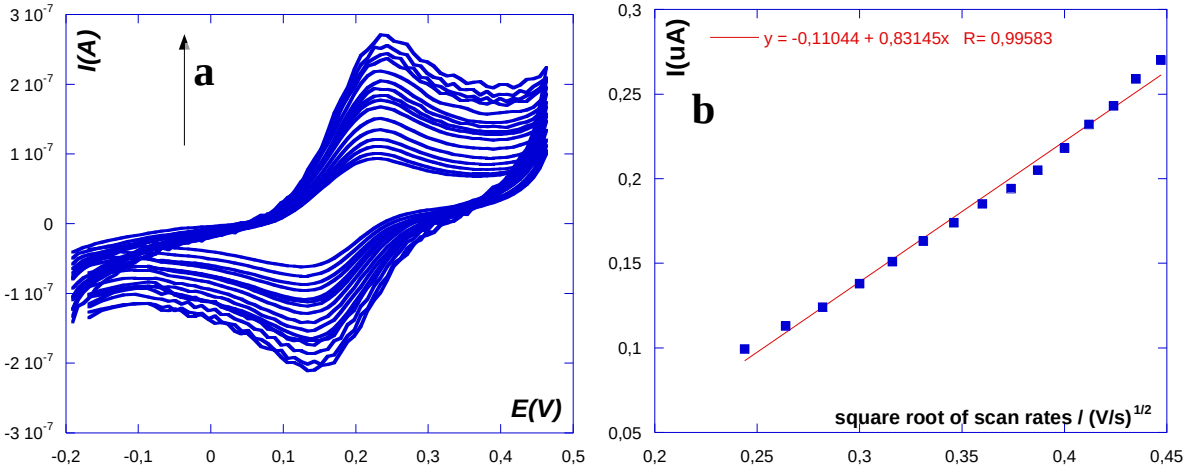

Fig. S4.2 (a) CV curves of the immunosensor with 141 ng/mL of HIgG at different scan rates from 50 to 170 mV/s in mQ water, (b): the linear dependence of oxidation peak current on the square root of the scan rates.

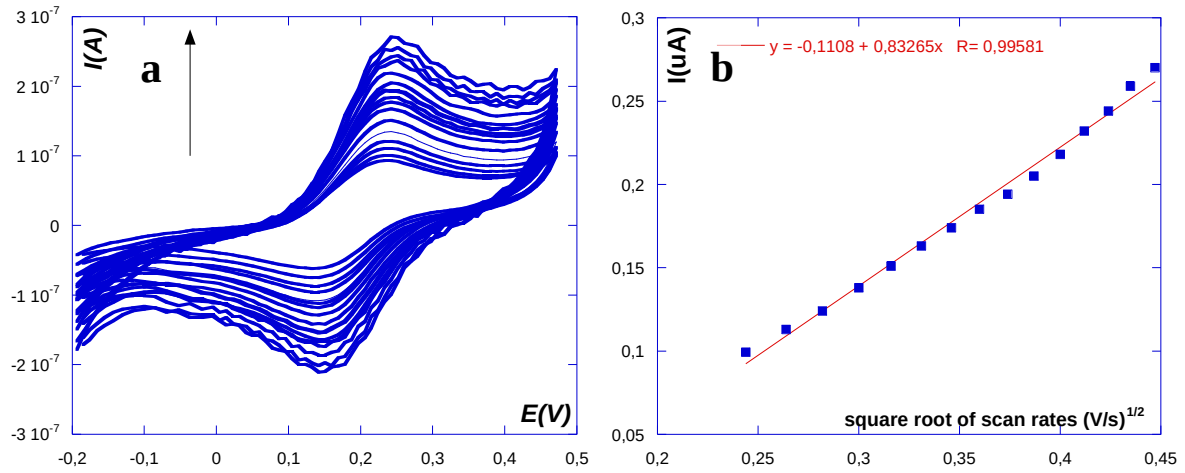

Fig. S4.3 (a) CV curves of the immunosensor with 188 ng/mL of HIgG at different scan rates from 50 to 170 mV/s in mQ water, (b): the linear dependence of oxidation peak current on the square root of the scan rates.

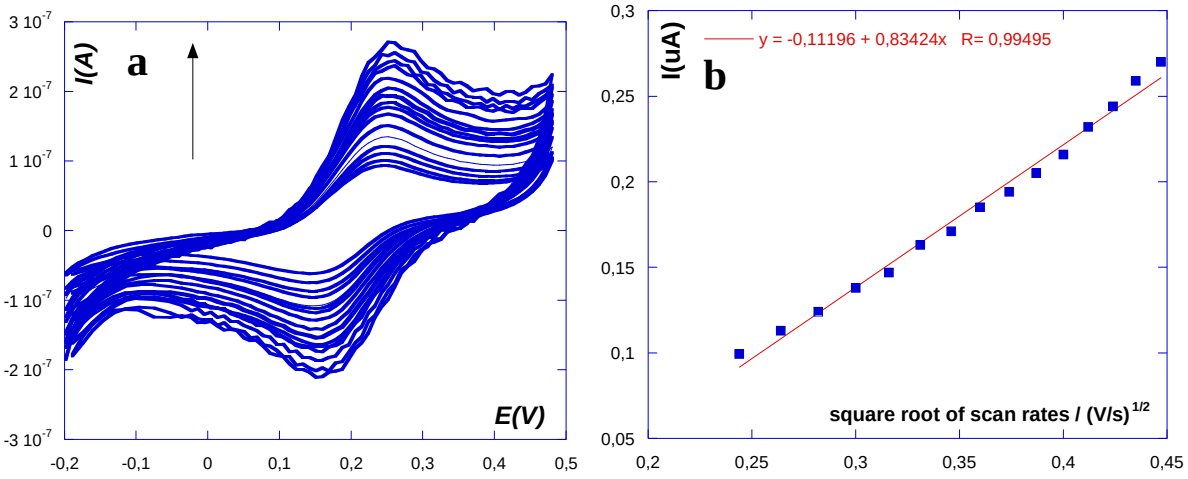

Fig. S4.4 (a) CV curves of the immunosensor with 235 ng/mL of HIgG at different scan rates from 50 to 170 mV/s in mQ water, (b): the linear dependence of oxidation peak current on the square root of the scan rates.

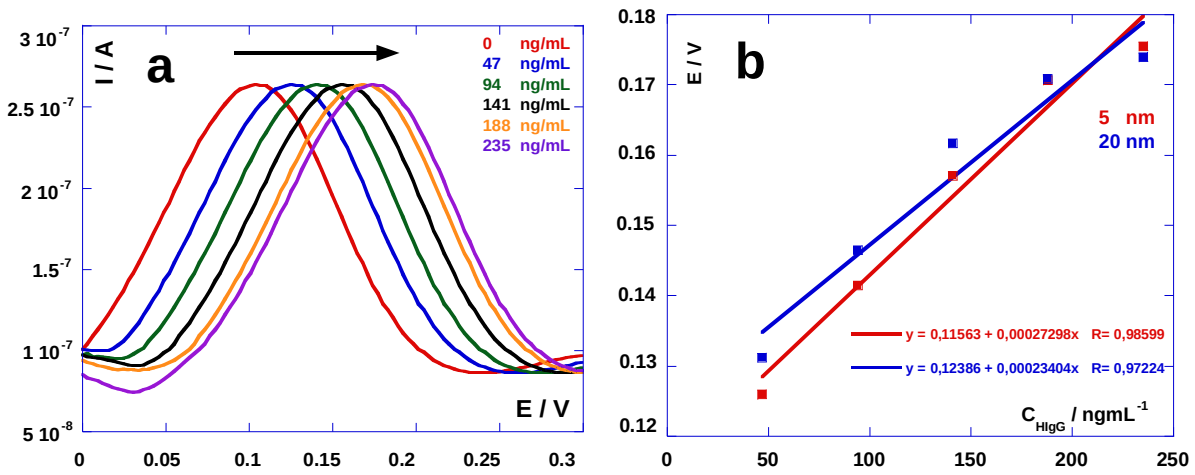

Fig. S5 DPV curves evidencing HIgG/αHIgG Ag/Ab recognition after progressive addition of HIgG (47 ng/mL each time) for 5 nm based immunosensor. (b) Comparison of potential variation versus added IgG amounts and fitting curves for 5 and 20 nm based immunosensors.

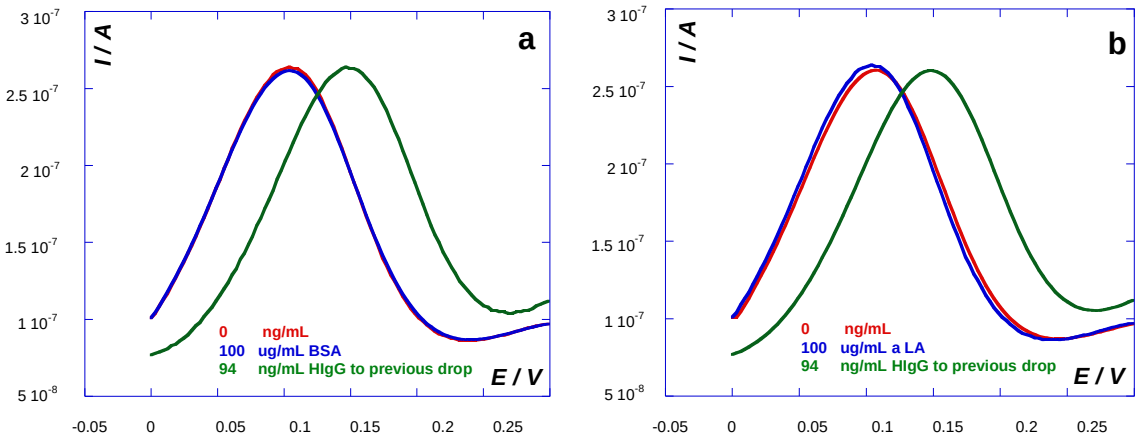

Fig. S6 selectivity study of the immunosensor response, (a) DPV response of HIgG immunosensor to the BSA protein, (b) DPV response of HIgG immunosensor to the αLA protein.

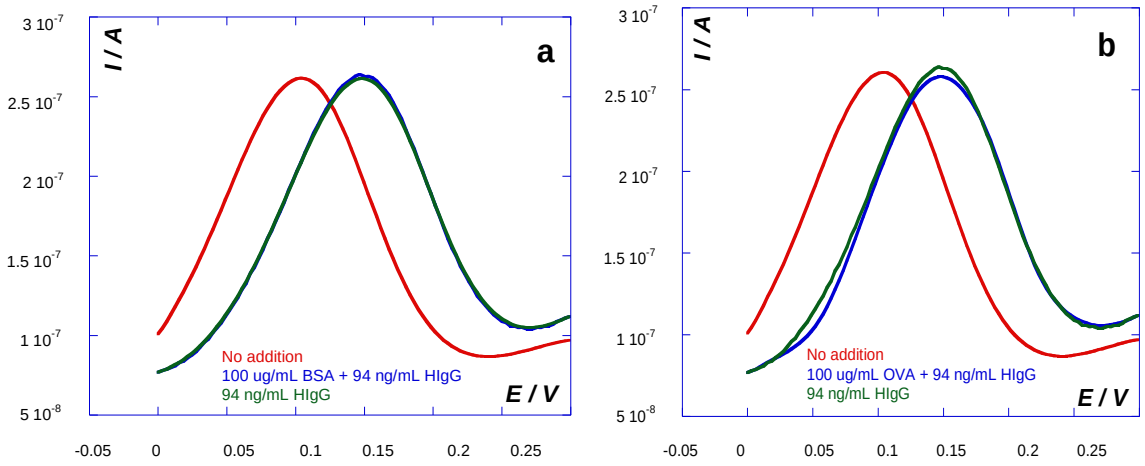

Fig. S7 specificity study of the immunosensor response, (a) DPV immunoresponse of HIgG sensor to the BSA protein, (b) DPV immunoresponse of HIgG sensor to OVA protein.